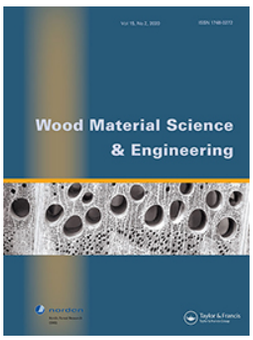

Wood Material Science & Engineering

ISSN: 1748-0272 (Print) 1748-0280 (Online) Journal homepage: https://www.tandfonline.com/loi/swoo20

Mechanical properties of natural fiber composites produced using dynamic sheet former

Liva Pupure, Janis Varna, Roberts Joffe, Fredrik Berthold & Arttu Miettinen

To cite this article: Liva Pupure, Janis Varna, Roberts Joffe, Fredrik Berthold & Arttu Miettinen (2020) Mechanical properties of natural fiber composites produced using dynamic sheet former, Wood Material Science & Engineering, 15:2, 76-86, DOI: 10.1080/17480272.2018.1482368

To link to this article: https://doi.org/10.1080/17480272.2018.1482368

Published online: 04 Jun 2018.

WOOD MATERIAL SCIENCE & ENGINEERING
2020, VOL. 15, NO. 2, 76–86
https://doi.org/10.1080/17480272.2018.1482368

Taylor & Francis
Taylor & Francis Group

Mechanical properties of natural fiber composites produced using dynamic sheet former

Liva Pupure[a], Janis Varna[a], Roberts Joffe[a,b], Fredrik Berthold[c] and Arttu Miettinen[d,e,f]

[a]Division of Materials Science, Luleå University of Technology, Luleå, Sweden; [b]Swerea SICOMP, Piteå, Sweden; [c]Rise Bioeconomy/Innventia AB, Stockholm, Sweden; [d]Department of Physics, University of Jyväskylä, Jyväskylä, Finland; [e]Swiss Light Source, Paul Scherrer Institute, Villigen, Switzerland; [f]Centre d'Imagerie BioMédicale, École Polytechnique Fédérale de Lausanne, Lausanne, Switzerland

ABSTRACT

Composites formed from wood fibers and man-made cellulosic fibers in PLA (polylactic acid) matrix, manufactured using sheet forming technique and hot pressing, are studied. The composites have very low density (due to high porosity) and rather good elastic modulus and tensile strength. As expected, these properties for the four types of wood fiber composites studied here improve with increasing weight fraction of fibers, even if porosity is also increasing. On the contrary, for man-made cellulosic fiber composites with circular fiber cross-section, the increasing fiber weight fraction (accompanied by increasing void content) has detrimental effect on stiffness and strength. The differences in behavior are discussed attributing them to fiber/ fiber interaction in wood fiber composites which does not happen in man-made fiber composites, and by rather weak fiber/ matrix interface for man-made fibers leading to macro-crack formation in large porosity regions.

ARTICLE HISTORY
Received 3 April 2018
Revised 23 April 2018
Accepted 23 May 2018

KEYWORDS
Wood fiber composites; PLA; Tencel fibers; dynamic sheet former; stiffness; strength

Introduction

The recent recognition of how our actions are affecting climate and nature is forcing us to use more environmentally friendly materials. Research on natural fiber composites has been in focus for recent years, due to their recyclability, renewability and good mechanical properties (Bledzki and Gassan 1999, Wambua *et al*. 2003). One of the latest trends is to use bio-based resin as a matrix, in order to have fully bio-based composites (Du *et al*. 2014, Fekete *et al*. 2018, Raghu *et al*. 2018). Wood plastic composites (WPC) have been one of the main research areas for bio-based composites (Bledzki and Gassan 1999, Eichhorn *et al*. 2001). The most common manufacturing methods for WPC is injection molding or extrusion (Migneault *et al*. 2009), but these methods damage fibers, by reducing fiber length in the process (Nyström 2007). Using manufacturing methods employed in paper making industry – wet forming of fiber sheets and compression molding – offers alternative manufacturing method, where fiber length is not affected.

It is not only the fiber length distribution that changes during extrusion process: fibers still have rather large aspect ratio. As shown by Gamstedt (1997) and Neagu (2006), fiber wall material is damaged and walls have collapsed resulting in fibers with lower stiffness and strength. It is expected that the dynamic sheet forming will introduce less damage on fibers because they are subjected only to compression transversely to the fiber orientation plane. Nevertheless, fiber failure in bending and collapsing fiber walls (in case of wood fibers with large lumen) is still expected.

Most common wood fiber reinforced polylactic acid (PLA) composites made by extrusion or injection molding have weight content of fibers 20–40% and elastic modulus in the range of 2–6.7 GPa whereas the tensile strength is in the order of 35–60 MPa (Bajpai *et al*. 2014, Spiridon *et al*. 2016, Mertens *et al*. 2017, Raghu *et al*. 2018). The experimental values for wood- and man-made cellulosic fiber composites presented in this paper have higher values. Due to very high porosity, the density of the discussed materials is very low, see Materials and Experimental Procedures section, and when stiffness and strength with respect to density are compared (specific properties) the composites presented in this paper are by far superior to conventional wood fiber composite materials.

The aim of this paper is to discuss the observed differences in mechanical behavior between composites made of different fiber types and its change with increasing fiber fraction and porosity content. Possible governing mechanisms are suggested based on microstructure of the composites and fracture surface inspection using scanning electron microscope (SEM) and X-ray computed tomography (CT). Rather accurate rule-of-mixtures (ROM) type engineering expressions with fiber length correction factors from shear lag analysis and orientation efficiency factors calculated from fiber orientation distribution developed by Krenchel (1964) have been previously used for short fiber composites. Since these models, assuming short fiber with a perfect interface completely embedded in a matrix, fail for composites with considerable void content, models of the same type have been modified to account for large porosity content in Madsen and Lilholt (2003) and Madsen *et al*. (2009, 2011). In

CONTACT Liva Pupure liva.pupure@ltu.se

this paper, it is demonstrated that the elastic properties of man-made cellulosic fiber composites are in-between the predictions of the two shear lag models (void-free and accounting for porosity) which are an expected behavior.

However, in spite of high porosity the experimental elastic modulus of wood fiber composites is not only higher than in the model accounting for porosity; the modulus is higher than it should be according to the shear lag model with perfect interface and no voids. Obviously, there should be another stiffening mechanism in wood fiber composites manufactured using methods of paper industry: fiber/fiber interaction which is also the main contributor to paper stiffness. In paper the collapsed (in transverse direction), band like shape of processed wood fibers enhance the probability of direct fiber–fiber interactions in the network compared to networks made using fibers of regenerated cellulose. The same distinction between wood fiber composites and man-made composites with fibers of circular cross-section can be made. In the latter, the fiber/fiber interaction is insignificant and the fiber/matrix interface is weak, as is discussed while interpreting the tensile strength data below. Results show that high void content, which is very detrimental for strength and stiffness of man-made cellulosic fiber composites, is of much less importance in wood fiber composites.

It is anticipated that the discussion in this paper will help to understand the potential and limitations of using high porosity cellulosic fiber composites.

Materials and experimental procedures

Constituents

Types of cellulosic fibers used in this study and their providers are listed in Table 1. Apart from bleached birch and softwood fibers, eucalyptus fibers and manmade cellulosic fiber (Lyocell Tencel) with four different configurations were used.

The STFI FiberMaster equipment and software were used for statistical analysis of fiber length and "width" distributions. Measurements were performed on ~0.1 g of slushed fibers (~10,000 fibers) before adding PLA fibers (see section about Composites Manufacturing). The average values from the FiberMaster data and the calculated fiber length/width aspect ratios are given in Table 1. For Tencel fibers, the width is the diameter (because of circular cross-section) and the ratio of diameters for 2.4 dtex and 1.7 dtex fibers calculated from data in Table 1 is 1.14 which is in a reasonably good agreement with radius ratio 1.19 obtained from linear densities. Diameters of 4- and 6-mm-long 1.7 dtex Tencel fibers were not measured; the diameter is expected to be the same as for 1.7 dtex 3 mm fibers and the length very close to 4 and 6 mm, respectively. More detailed data regarding fiber length distribution and fiber width distribution are presented in Figure 1 and discussed in Results and Discussions section.

PLA in a fiber form from Unitika, Japan (PLo1, 1.7 dtex (linear density) with 5 mm length), was used as a matrix material. According to Madhavan Nampoothiri *et al.* (2010), the density of PLA is between 1.25 and 1.43 g/cm^3, close to wall density of natural fibers (see Table 1). Since the density of PLA is similar to the density of Tencel fibers, the 1.7 dtex PLA fibers should have similar diameter as 1.7 dtex Tencel fibers, see Table 1.

Composites manufacturing

Composites with weight fraction of fibers 40% and 60% were manufactured. Sheets from fibers listed in Table 1 were produced using a dynamic sheet former. Eucalyptus fibers were pulped using standard sulfate pulping conditions in laboratory at MoRe and Innventia from chips.

In order to ensure good swelling, cellulosic fibers were slushed the day before sheet production. Before formation of the sheet, the slushed PLA fibers were added to the mix. Reslushing of pulps was done using British pulp evaluation apparatus (BPEA, Mavis engineering Ldt) with 2000 turns. The dynamic sheet former was used with 1300 rpm rotation speed and 300 kPa spray pressure. Directly after removal from the drum, fresh sheets were pressed, cut into three pieces and dried on a warm plate, set to 40°C for 1 h under restrain. The surface density of the produced dynamic sheets was close to 240 g/m^2.

For each composite, five pre-dried sheets were placed within a 1-mm-thick frame on a metal plate covered with polyethylene terephthalate (PET) film. The dynamic sheet forming induces anisotropy in the sheet so that the mechanical properties in the machine (MD) and cross machine (CD) directions are different. Therefore, making the stack of sheets, care was taken to align all sheets in MD direction. After placing the sheets in the frame a second PET film and an upper metal plate were put on the top of the stack and the whole assembly was kept for 1 h in an oven (110°C) and then moved to the standard planar press (Servi.Tec Polystat 200 T equipped with water cooling) heated to 185°C. Enough pressure was applied to ensure complete closure of the press tool. All samples were pressed for 20 min to ensure complete melting of the PLA component. Earlier experiments had showed that PLA completely melts after much shorter time than 20 min. Cooling was done under

Table 1. Fiber types and their characteristics.

Fiber type	Provider	Length (mm)	Width (μm)	Aspect ratio	Fiber modulus (GPa)	Wall density (g/cm^3)
Birch	Botnia, FI	0.886	22.9	38.7	10–70[1,2]	1.47*
Softwood	Södra, SE	2.004	30.8	65.1	3.1–50[2,3]	1.50*
1.7 dtex 3 mm Tencel	Lenzing, GE	3.034	22.4	135.4	10–30.5[4,5]	1.50[4,5]
1.7 dtex 4 mm Tencel	Lenzing GE	–	–	–	10–30.5[4,5]	1.50[4,5]
1.7 dtex 6 mm Tencel	Lenzing, GE	–	–	–	10–30.5[4,5]	1.50[4,5]
2.4 dtex 6 mm Tencel	Lenzing, GE	5.915	25.5	232.0	10–30.5[4,5]	1.50[4,5]
Eucalyptus viminalis	Innventia, SE	0.720	20.8	34.6	30–43[1]	1.50*

[1]Neagu *et al.* (2006); [2]Lilholt and Lawther (2000); [3]Mott *et al.* (2002); [4]Adusumali *et al.* (2006); [5]Abdennadher *et al.* (2016).
*Assumed based on Kellogg and Wangaard (1969).

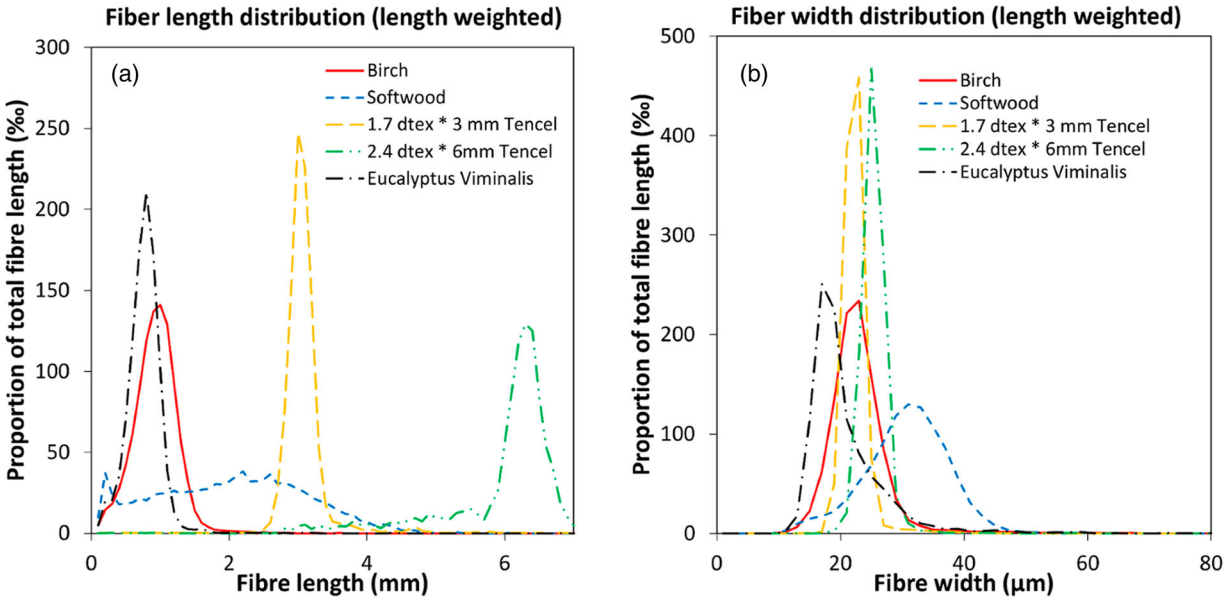

Figure 1. Fiber (a) length distribution and (b) width distribution.

maintaining pressure until the tool reached 40°C so that all samples had similar heat history. Additionally, cooling to below T_g of PLA ensures that samples do not change shape when the press tool is opened.

After removing the composite from the hot press, it was observed that in some cases, the sheet material had stacked on the frame, thus not allowing the upper plate to completely close the mold. This is the main reason for thickness of the composite plates being larger than the thickness of the frame (1 mm) and for the large porosity analyzed in Results and Discussions section. This problem was larger for composites with higher fiber content.

Dog bone composite specimens were cut in the machine direction from plates using water-jet cutting. The final dimensions of specimens were with thickness about 1–1.5 mm and with width of 13 mm in the working zone (length of the working zone was approximately 80 mm). Total length (including clamping parts) of the specimen was 160 mm and grip separation distance was 100 mm. Care was taken not to include material from the edge of the plates in the cut out dog bone samples.

Pure PLA plates were also manufactured using the same parameters. They were cut in rectangular shape samples with approximate dimensions: length 50 mm (working zone length 30 mm), thickness 0.4 mm and width 10 mm. Detailed specification of each composite is presented in Table 2. Composite density in Table 2 is calculated from the weight of the plate and its dimensions. Thus information regarding density of individual specimens is not available.

Experimental procedures

Tensile testing

Specimens were tested in tension along the machine direction. Quasi-static tensile tests were performed in displacement controlled mode at 10 mm/min (roughly corresponding to 10%/min) on Instron 3366 equipped with 10 kN load cell and pneumatic grips. Extensometer 2620-601 with 50 mm base was used to measure axial strain. Elastic modulus was determined from the slope of the stress–strain curve in the linear strain region 0.05–0.3%. All tests were performed at room temperature and humidity. From each type of composite, five specimens were tested.

Tensile tests (displacement rate 3 mm/min corresponding to approximately 10%/min) with a goal to find elastic modulus and stress/strain to failure were performed on rectangular PLA specimens. Universal testing machine Shimadzu AG-X was used and strain was measured using video-extensometer Shimadzu DVE 201. The strength data for PLA were not reliable due to premature failure of specimen in the grips. Nevertheless, at least 60 MPa stress was reached in all these tests. The elastic modulus of PLA determined from these tests is approximately 2.9 GPa, which is in agreement with data presented by Du *et al.* (2014).

Porosity studies

Void content in the composite was estimated from the measured and theoretical density of the composite as described in Results and Discussion section. Detailed investigation of volume fraction of pores and their statistical

Table 2. Density of composites.

Fiber type	Fiber weight fraction W_f (%)	Plate thickness (mm)	Density (g/cm^3)
Birch (bleached)	60	1.23	1.02
	40	1.12	1.10
Softwood (bleached)	60	1.19	1.04
	40	1.11	1.14
1.7 dtex·3 mm "Tencel"	60	1.17	1.11
	40	1.17	1.08
1.7 dtex·4 mm "Tencel"	60	1.20	1.02
	40	1.08	1.14
1.7 dtex·6 mm "Tencel"	60	1.38	0.93
	40	1.16	1.12
2.4 dtex·6 mm "Tencel"	60	1.50	0.89
	40	1.11	1.16
Eucalyptus viminalis	60	1.33	0.92
	40	1.06	1.18

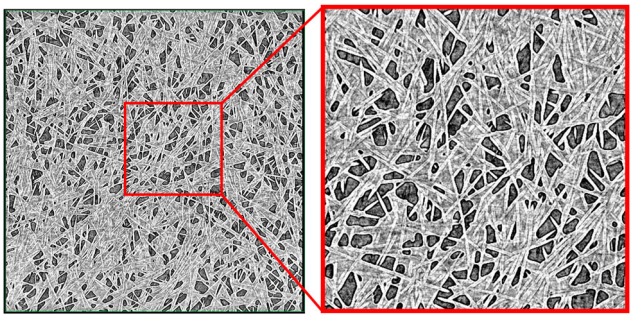

Figure 2. In-plane section of Tencel fiber (60%)/PLA composite: circular fibers are partially covered with PLA matrix creating a network with very large void content. Area on the left is 3 × 3 mm and fiber diameter is 25.5 µm.

characteristics was performed using CT equipment Zeiss Xradia 510 Versa. An example of a CT image (30% void content) is shown in Figure 2.

The CT images were segmented using a machine learning-based segmentation tool (Arganda-Carreras *et al*. 2017). Fiber orientation and pore diameter distributions were determined from the segmented data using the structure tensor method (Jähne 2004) and opening transform (Hildebrand and Rüegsegger 1997), respectively. Example of the results in Figure 3 shows that the distribution of fibers is not random and that the variation in pore size is huge, some of the pores reaching 50 microns in diameter which is more than twice the fiber diameter. Only one small cylinder of each composite with diameter and length 3 mm was scanned.

SEM fracture surfaces

SEM (JEOL, JSM-5200, low vacuum, acceleration tension 20 kW) was used to analyze fiber breaks, interface quality and collapsed fiber shapes on composites fracture surfaces. One specimen of each composite was analyzed.

Results and discussions

Volume fractions and geometrical parameters of constituents

The length and width distributions for softwood in Figure 1 are much wider than for other fibers. This is consistent with FiberMaster data regarding fines (to be considered in analysis as particles rather than fibers) in this material (12.4%). The corresponding number is about 4% for the rest of natural fibers and 0.3% for Tencel fibers. One can expect that in composite these "particles" will not contribute to stiffness more than the matrix. Softwoods such as spruce naturally have a broader fiber length distribution compared to hardwood fibers (Sjöström 1993). In most cases, a clear separation between distributions for different fiber types was observed. The eucalyptus species were significantly shorter and slimmer than the other fiber types studied.

It was expected that in contrast to extrusion techniques, fibers in the used manufacturing procedure would not be damaged. However, Figure 4(a–c) shows that most of the natural fibers with lumen have collapsed in the thickness direction: the lumen is hardly visible. This means that the axial fiber properties, indeed, may be not much degraded but the transverse are especially in the composite thickness direction.

For any composite material, the volume fractions of constituents can be determined from weight fractions (known from manufacturing) provided the density of the composite is measured and densities of constituents are known. Using mass conservation law $m_c = m_f + m_m$, the very well-known expressions, valid also for highly porous materials, are obtained

$$V_f = W_f \frac{\rho_c}{\rho_f}, \quad V_m = W_m \frac{\rho_c}{\rho_m}. \tag{1}$$

In (1), indexes *c, f, m* denote the composite, fibers and matrix, respectively, W is the weight content and V is the volume content. Obviously the porosity characterized by void volume content is obtained as

$$V_v = 1 - V_f - V_m. \tag{2}$$

Using the composite density from Table 2 and the fiber wall density from Table 1, the volume fractions given in Table 3 were calculated.

The void content is very high and it dramatically increases when the weight content of fibers was changed from 40% to 60%. There are no obvious trends in void content in composites made from different fibers.

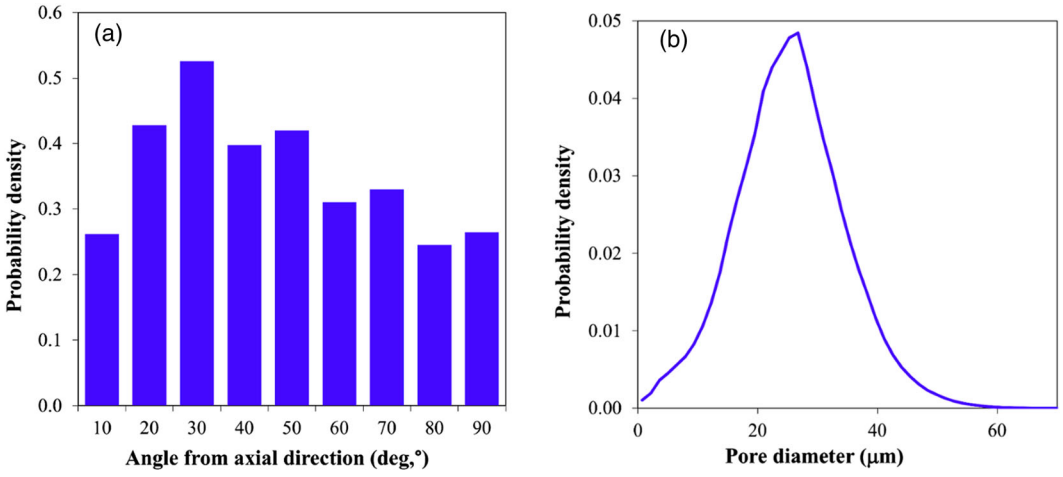

Figure 3. Statistical characteristics of Tencel/PLA composite: (a) fiber orientation distribution; (b) pore size distribution.

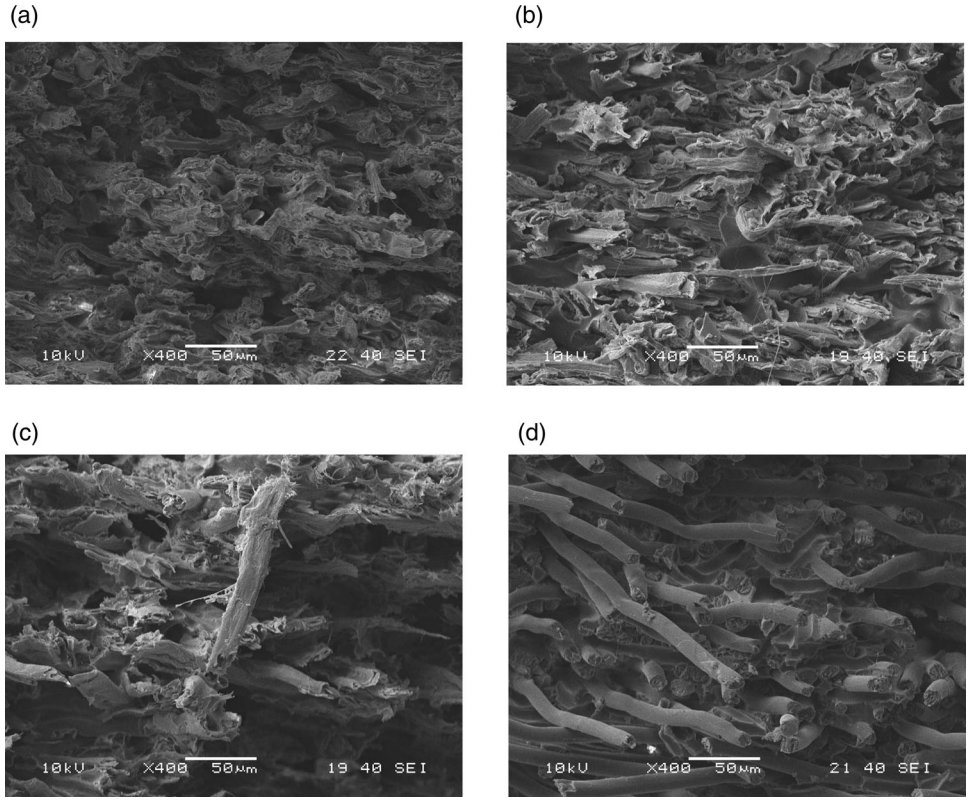

Figure 4. SEM micrographs of fracture surface details for some composites: (a) birch with $W_f = 60\%$; (b) birch with $W_f = 40\%$; (c) softwood with $W_f = 60\%$; (d) Tencel 1.7 dtex 3 mm $W_f = 60\%$.

It should be noted that in practical application, Equation (2) can be rather inaccurate for cases with low void content, which fortunately was not a problem in this paper. Nevertheless, in order to validate values in Table 3, volume content measurements on some composites were performed using CT tomography, see section about Experimental Procedures. The investigated volume in CT is rather small (the diameter and the length of the scanned cylinder was 3 mm) comparing with the plate used for Table 2 and therefore some deviations from average are inevitable. The local values ($V_v = 0.281$, $V_f = 0.491\%$, $V_m = 0.228$) obtained with CT for one cylinder with 60% 2.4 dtex 6 mm Tencel fibers are slightly different than the averages for composite plate in Table 3, but the agreement can be considered as good and the values in Table 3 as representative.

Four high-resolution examples of the composites fracture surface are shown in Figure 4 showing: (a) smoother fracture surface of composite with 60% weight content birch comparing with (b) 40% birch (more brittle macroscopic behavior in 60% case is typical for high stress failure); (c) more pull-outs for softwood comparing with birch; (d) circular Tencel fibers with smooth and "clean" surface (weak interface) and with much longer fiber ends than for other composites.

In wood fiber composites, fibers have a lumen which could be responsible for some part of the porosity when density is used to determine the void content. However, according to Figure 4 most of the pulp fibers have collapsed due to the high compression during manufacturing and, hence, contribution of the lumen to the porosity is not very significant. The high porosity is not visible in these cross-sections, which indicate that the main plane of these voids is mostly parallel to the composite midplane.

Table 3. Volume fraction of voids, fibers and PLA matrix in composites.

	$W_f = 40\%$			$W_f = 60\%$		
Fiber type	V_v	V_f	V_m	V_v	V_f	V_m
Birch	0.19	0.30	0.51	0.27	0.42	0.31
Softwood	0.17	0.30	0.53	0.26	0.42	0.32
1.7 dtex 3 mm Tencel	0.21	0.29	0.50	0.21	0.44	0.34
1.7 dtex 4 mm Tencel	0.17	0.30	0.53	0.28	0.41	0.31
1.7 dtex 6 mm Tencel	0.18	0.30	0.52	0.34	0.37	0.29
2.4 dtex 6 mm Tencel	0.16	0.31	0.54	0.37	0.36	0.27
Eucalyptus viminalis	0.14	0.31	0.55	0.35	0.37	0.28

Tensile test results

In Figure 5, stress–strain curves for the most representative specimen of each composite are presented. The behavior for all composites is rather linear until 0.6% strain. The source of the inelastic behavior at higher strains was not investigated: it could be a combination of viscoplasticity and viscoelasticity typical for natural fiber composites (Marklund *et al.* 2006, Varna *et al.* 2012, Pupure *et al.* 2013). Average values from tensile tests and standard deviations are presented in Table 4. There are differences in the "elastic" region in Figure 5(a) for natural fiber composites, but for the same type of composite the response is always stiffer with increasing fiber weight content. In the inelastic region, the nonlinear response is rather similar for both weight fractions and the difference is due to stress "gain" in

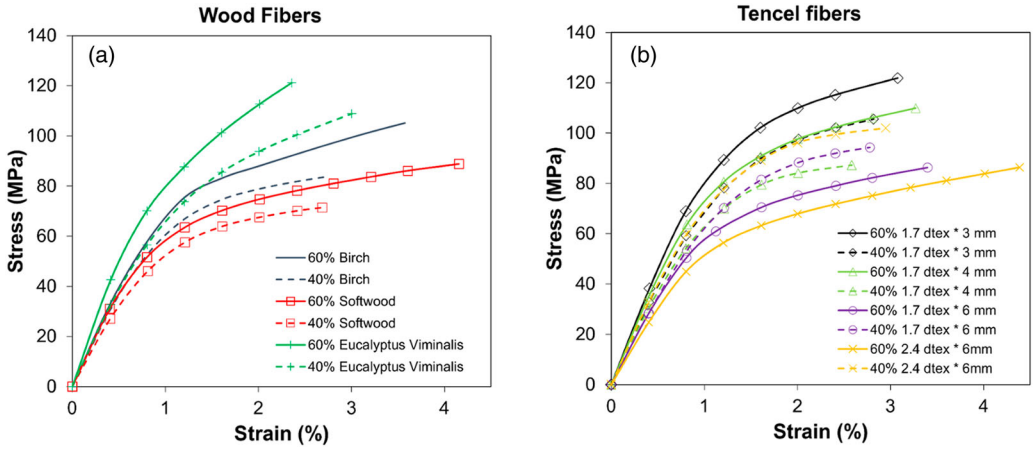

Figure 5. Stress–strain curves for composites with (a) wood fibers, (b) Tencel fibers.

the "elastic" region. A closer look shows that in the inelastic region the gap between curves for different weight fractions is slightly increasing, indicating that the nonlinearity is mostly due to inelastic PLA behavior not studied separately in this work.

The behavior of Tencel fiber composites in Figure 5(b) is very peculiar. For 1.7 dtex fibers with length 3 and 4 mm trends are the same as for wood fibers in Figure 5(a): with increasing fiber weight fraction the stress response is higher. The gap between stress curves in the inelastic region increases with strain indicating that the inelastic behavior mostly depends on matrix (man-made "natural" fibers could also be very inelastic with distinct plastic and viscoplastic strains as shown by Pupure *et al.* (2014, 2015)). Tests on twisted and untwisted Tencel fiber tows presented by Abdullah *et al.* (2006) showed that the stress response in tensile loading is rather linear until 1.5% strain. Starting with 2% strain, the stress–strain curve is still almost linear but the slope is several times lower and, finally, fibers break at about 7% strain (untwisted bundles).

In Figure 5(b), composite stresses at any given strain are higher in the composite with shorter (3 mm) fibers which contradicts all available knowledge regarding the fiber aspect ratio effect on short fiber composites behavior (Agarwal and Broutman 1990). However, for fairness it should be noted that according to Table 1 all fibers can be treated as long fibers, provided the stress transfer over the interface is good, in the context of stress transfer length (more details are given in Discussion section where modeling approaches to the elastic response are analyzed).

Both 6 mm Tencel fiber composites showed unexpected behavior:

- The elastic modulus is lower for higher (60%) fiber weight fraction composite.
- In the inelastic region, stresses are much higher for 40% than for 60% composite.
- The detrimental effect of increasing weight fraction on increase of stress is larger for composites with thicker fibers (2.4 dtex).

In the inelastic region, the behavior of both 6 mm 40% Tencel fiber composites is more inelastic than the behavior of 60% composites: the gap between curves corresponding to the two weight fractions decreases indicating that matrix inelasticity is dominating. To verify the above-described behavior of Tencel fiber composites, new plates of these composites were manufactured and tested. Experiments showed the same peculiar trend: the modulus of both 6 mm Tencel composites was lower when the fiber weight fraction was 60%: 29% reduction for 1.7 dtex and 35% reduction for 2.4 dtex Tencel composites.

Table 4. Mechanical properties of composites. Standard deviation is presented in ( ).

Notation	Fiber type (weight fraction)	Elastic modulus (GPa)	Max stress (MPa)	Strain at max stress (%)
1	Birch, $W_f = 60\%$	8.8 (0.4)	103.3 (5.3)	3.64 (0.33)
2	Birch, $W_f = 40\%$	7.2 (0.6)	79.3 (7.7)	2.80 (0.24)
3	Softwood, $W_f = 60\%$	8.2 (0.5)	91.6 (5.0)	3.92 (0.28)
4	Softwood, $W_f = 40\%$	6.6 (0.2)	70.9 (2.5)	2.59 (0.26)
5	1.7dtex·3 mm Tencel, $W_f = 60\%$	9.6 (0.9)	124.6 (13.6)	3.33 (0.21)
6	1.7dtex·3 mm Tencel, $W_f = 40\%$	8.1 (0.3)	98.1 (7.2)	2.51 (0.57)
7	1.7dtex·4 mm Tencel, $W_f = 60\%$	8.4 (0.4)	110.6 (2.9)	3.49 (0.48)
8	1.7dtex·4 mm Tencel, $W_f = 40\%$	7.3 (0.2)	89.0 (1.8)	2.27 (0.27)
9	1.7dtex·6 mm Tencel, $W_f = 60\%$	6.7 (0.2)	86.5 (4.5)	3.68 (0.61)
10	1.7dtex·6 mm Tencel, $W_f = 40\%$	7.4 (0.4)	94.0 (1.4)	2.96 (0.18)
11	2.4dtex·6 mm Tencel, $W_f = 60\%$	6.4 (0.5)	85.5 (5.9)	4.42 (0.15)
12	2.4dtex·6 mm Tencel, $W_f = 40\%$	8.0 (0.2)	101.1 (3.2)	2.90 (0.18)
13	*Eucalyptus viminalis*, $W_f = 60\%$	10.7 (0.3)	130.2 (13.6)	2.49 (0.40)
14	*Eucalyptus viminalis*, $W_f = 40\%$	7.9 (0.8)	105.6 (5.5)	3.06 (0.26)

Average values of the elastic modulus (defined as described in section about Experimental Procedures), the maximum stress and the strain at maximum stress are presented in Table 4. Main trends will be discussed in the next section.

Discussion

As shown in Table 1, the variation in elastic modulus of natural fibers of one specific kind is so large that analysis with a goal of comparing different types of composites is impossible unless fiber testing of the fibers used in this specific composite is performed. Since fiber modulus and strength distributions are not available, we will focus on explaining differences in the same type of composites due to two different weight contents used. Moreover, because the fiber orientation distribution with respect to machine direction in $W_f = 60\%$ and in $W_f = 40\%$ composites could be different, the analysis and the explanations provided in this section should be considered as indicative only.

Elastic modulus

Wood fiber composites. Elastic modulus data from Table 4 are normalized with respect to the modulus value at $W_f = 40\%$ and shown in Figure 6. As expected, the elastic modulus of wood fiber composites increases with increase of the fiber weight fraction. In fact, as follows from micromechanics it is not the weight fraction but rather the volume fraction that is decisive for elastic modulus of a composite and, therefore, volume fraction data in Table 3 has to be used in discussion.

All simplest micromechanics models claim that the composite modulus is proportional to the fiber volume fraction. Results in Table 5 for wood fiber composites confirm that there is a correlation. However, the stiffening effect is the largest for eucalyptus composite where the V_f increase is the smallest.

Using Krenchel's model (1964), which is one of the most commonly used models for short nonaligned fiber composites, the composite modulus is

$$E_c = E_f \eta_l \eta_\theta V_f + E_m V_m. \tag{3}$$

In (3), η_θ is orientation efficiency factor, η_l is the so-called length correction factor defined as

$$\eta_l = 1 - \frac{2}{\beta l}\tanh\frac{\beta l}{2}, \tag{4}$$

$$\beta = \frac{1}{r_f}\sqrt{\frac{4G_m}{E_f \ln(1/V_f)}}. \tag{5}$$

G_m is matrix shear modulus, r_f is fiber radius and l is the fiber length. Expression (3) follows from purely mathematical derivation showing that the applied stress can be written as a ROM of average stresses in constituents and therefore it is applicable also in presence of voids (with zero average stress in the void). Using the data in Table 1 and matrix shear modulus 1 GPa the calculated length correction factor for all wood composites is ≈ 1 and, hence, fibers can be considered as "long". Note that the length correction factor expression comes from a shear lag model for a short fiber embedded in a matrix with perfect bond at the fiber/matrix interface. According to Table 3 and Figure 2, the porosity at $W_f = 60\%$ is so high that the fiber cannot be considered as "embedded" and, therefore, the shear lag model may be not applicable, strongly overestimating the elastic modulus.

The orientation efficiency factor η_θ may be calculated from orientation distribution like the one shown in Figure 3(a). For random in-plane fiber distribution $\eta_\theta = 3/8$. Since the fiber modulus is not known and the orientation distribution values were experimentally evaluated for only one composite (Figure 3), the applicability of (3) was checked in the following way (assuming the same fiber orientation distribution at both weight contents): experimental data for $W_f = 40\%$ and (3) were used to calculate $E_f \cdot \eta_\theta$ which were used in (3) to calculate composite modulus at $W_f = 60\%$. Results are presented in Table 6.

The shear lag model (3)–(5) assumes perfect bonding between fiber and matrix in a composite where fibers are surrounded by matrix continuum without any large pores. To account for porosity, the above model was modified by introducing one more correction term, leading to the following expression for composite elastic modulus (Madsen and Lilholt 2003, Madsen *et al.* 2009, 2011)

$$E_c = (E_f \eta_l \eta_\theta V_f + E_m V_m)(1 - V_v)^2. \tag{6}$$

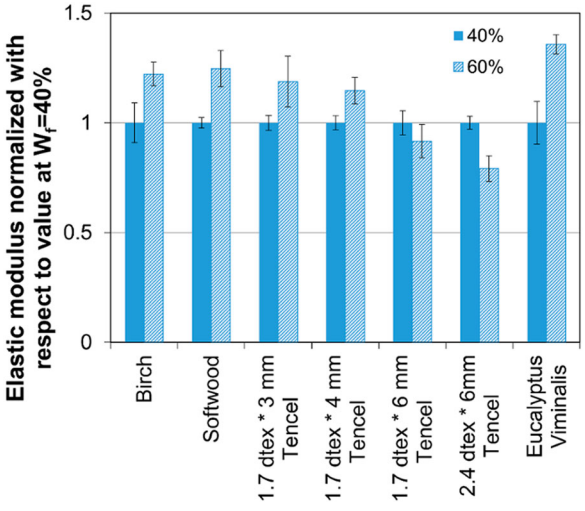

Figure 6. Elastic modulus data normalized with respect to modulus at $W_f = 40\%$ of the same fiber composite.

Table 5. Elastic modulus change with variation of fiber volume fraction change: wood fiber composites.

Fiber type	$V_f(60)/V_f(40)$	$E_c(60)/E_c(40)$
Birch	1.39	1.22
Softwood	1.37	1.24
Eucalyptus viminalis	1.19	1.35

Table 6. Elastic modulus of wood composites with $W_f = 60\%$.

Fiber type	E_c (GPa) experimental	E_c(GPa) shear lag m.	E_c(GPa) (Eq. 6)
Birch	8.8	8.9	7.6
Softwood	8.2	7.9	6.5
Eucalyptus viminalis	10.7	8.3	4.9

Authors have demonstrated the applicability of this expression for plant fiber/polypropylene and hemp and flax fiber/starch composites. Elastic modulus of wood fiber composites calculated according to (6) using the same procedure as described above for the shear lag model is also given in Table 6. The modulus values are significantly lower than the experimental and, as expected, lower than the shear lag model values not accounting r porosity. For eucalyptus composite, the difference is very large: the experimental value is more than two times larger than the calculated with the model accounting for porosity. The expectation was that the shear lag model with perfect bonding would overestimate the modulus and the expression (6) with porosity would be closer to test data. For all these composites, expression (6) predicts that the modulus at $W_f = 60\%$ will be equal or lower than at $W_f = 40\%$, which contradicts data in Table 4. In fact, the simple estimate that the composite modulus change is proportional to V_f change (Table 5) is the closest to reality.

The disagreement between theories and test shows that for these composites there are other stiffening mechanisms not included in the above two models. One of these mechanisms is interaction between wood fibers, which is the major phenomenon defining the stiffness of a paper: relatively large fiber surfaces are brought in contact by high pressure during composite manufacturing. Rather flat surfaces of these fibers, see Figure 4(a–c), makes the fiber/fiber contact surface large, enabling possibility for chemical bond between them. The relatively stiff and strong network of fibers contributes to the stiffness of the composite and leads to higher values than calculated using fiber/matrix interaction only.

This phenomenon could be a possible explanation of the highest effect of V_f of eucalyptus fibers on composite modulus in Table 5: these fibers have the smallest "width" (Table 1) and, therefore, their bending stiffness is the lowest. During the applied pressure, these thin fibers are more compliant and they find more contacts with other fibers than thick fibers do. In addition, shorter fibers can easily accommodate in the composite to have more contact with other fibers. These could be the reasons for the highest E_c of eucalyptus among the wood composites at $W_f = 40\%$. It also results in high effect on modulus of modestly increasing V_f in Table 5 (fibers are finding larger total contact area).

Tencel fiber composites. Similar investigation of Tencel composites, see Table 7, shows much smaller stiffening effect of increasing V_f on composite modulus. For 6-mm-long fibers, the effect of V_f is even opposite to the expected. Shorter fiber composites, see Figure 7, have larger elastic modulus.

The shear lag model (3)–(5) was applied using the same procedure as for wood fiber composites predicting elastic modulus at $W_f = 60\%$ based on test data for $W_f = 40\%$. In contrast to wood, the predicted shear lag model values presented in Table 8 are always higher than the experimental. The void content in 3 mm composite was the same in 40% and 60% case and it cancels out when (6) is used for these two weight contents. Therefore, applying the model with porosity (6) to the 3 mm composite, predictions for $W_f = 60\%$ in Table 8 based on E_c value at $W_f = 40\%$ are very similar as in shear lag model (3)–(5). In all other composites, the void content significantly changes with fiber weight fraction and applying (6) the predicted modulus, see Table 8, is always lower than the experimental.

Table 7. Elastic modulus change with variation of fiber volume fraction change: Tencel fiber composites.

Fiber type	$V_f(60)/V_f(40)$	$E_c(60)/E_c(40)$
1.7 dtex 3 mm Tencel	1.54	1.19
1.7 dtex 4 mm Tencel	1.34	1.15
1.7 dtex 6 mm Tencel	1.25	0.91
2.4 dtex 6 mm Tencel	1.15	0.80

This is what may be expected when fiber/matrix interaction and porosity are the main stiffness determining phenomena. In other words, it seems that the effect of fiber/fiber interaction (if any) is much smaller for these composites. It makes sense because Tencel fibers have circular cross-section, see Figure 4(d), and theoretically the contact area for touching nonaligned fibers is equal to zero.

Thus model (6) which accounts for porosity is able to predict the reduction of elastic modulus in 6-mm Tencel fiber composites with increasing W_f and also the larger modulus reduction in the 2.4 dtex composite.

Comparing the experimental and calculated modulus ratios in Tables 7 and 8, it seems that the detrimental effect of porosity on modulus in (6) is over-predicted when very high porosity levels as in this paper are used.

Strength

For proper analysis the strength in Table 4, defined as the maximum stress in the stress–strain curve, has to be analyzed as a function of V_f. Table 9 shows the fiber volume fraction change when weight fraction in wood fiber composites is changed from 40% to 60%; the void content change and the strength σ_c change. It is rather clear that the strength ratio roughly follows the volume fraction ratio.

The potential mechanisms leading to composite failure are: (a) breaking fibers oriented along the loading direction; (b) breaking the fiber network which means to break the fiber/fiber contact surface. For both mechanisms, when V_f increases

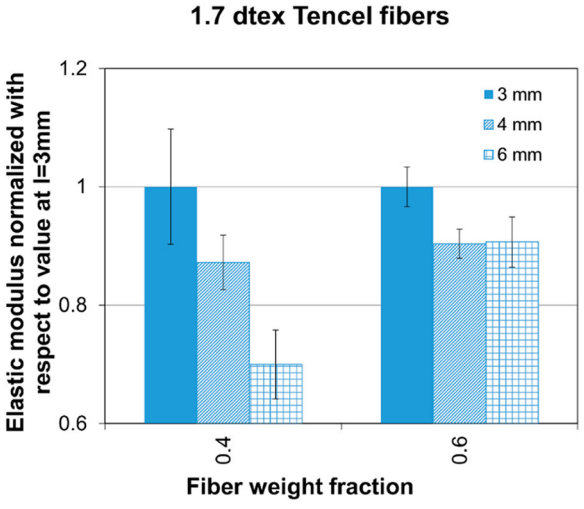

Figure 7. Elastic modulus of Tencel fiber composites normalized with respect to the modulus value for $l = 3$ mm composite.

Table 8. Elastic modulus of Tencel composites with $W_f = 60\%$.

Fiber type	E_c(GPa) experimental	E_c(GPa) shear lag m.	$E_c(60)/E_c(40)$ shear lag m.	E_c(GPa) (Eq. 6)	$E_c(60)/E_c(40)$ (Eq. 6)
1.7 dtex 3 mm Tencel	9.6	11.3	1.39	11.7	1.44
1.7 dtex 4 mm Tencel	8.4	8.7	1.19	6.8	0.93
1.7 dtex 6 mm Tencel	6.7	8.2	1.11	5.6	0.75
2.4 dtex 6 mm Tencel	6.4	8.2	1.03	4.7	0.59

a larger applied stress is required to trigger them. In these mechanisms, the void content change is less important, conclusion which is consistent with data in Table 9.

Another possible mechanism, that would be more probable when the fiber failure strain is large, the fraction of fibers oriented in the loading direction is small and when the fiber/matrix interface is weak, is a formation of a macrocrack with a plane transverse to the loading direction. It may form in the matrix by coalescence of multiple transversely loaded fiber/matrix debonds and voids. However, in wood fiber composites the interface strength is usually good and the fiber surface is not too smooth, making this failure triggering mechanism less probable. No signs of this mechanism can be found on fracture surfaces in Figures 4 (a–c), 8 and 9.

Figure 8 shows fracture surface of a softwood composite in which according to FiberMaster measurements 12.4% of all fibers are fines. Clustering of these fines shown in Figure 8 explains the lowest strength of this composite among all studied wood fiber composites.

The eucalyptus fibers, which are the shortest and tiniest, have the best ability to accommodate in the composite making the largest fiber/fiber contact surface which results in the highest strength among wood fiber composites.

In Tencel fiber composites, failure of fibers aligned with the load direction as a failure triggering mechanism is not probable: Tencel fibers break at about 7% strain as shown by Abdullah *et al*. (2006). Strength change of Tencel fiber composites with fiber volume fraction change is shown in Table 10. It seems that there is no correlation. Instead there seems to be a strong correlation with the void content change (especially for large change) also shown in Table 10.

In Tencel fiber composites, the fiber/fiber interaction is negligible. Fiber surface in Figure 10 is very clean: a strong indication that the interface is weak. It can be noticed that these fibers which appear to be pulled out from the material are not the ones aligned with the load. In fact, majority of them have off-axis orientation which makes fiber breaking and related pull-out impossible. It is possible that these fibers have been debonded from the matrix in combined transverse-shear loading. Debonding is a part of the process of creating a large crack running transverse to the loading direction through debonds, voids and matrix. The extensive breakage of these debonded fibers shown in Figures 10–12 may be due to bending of these crack bridging fibers in the final stage of the crack development. There is another group of broken fibers noticeable in Figure 10 with very short pull-outs and with orientation in the load direction. These fiber breaks may have resulted from very large local strains in fibers aligned with load who bridge the macroscopically opening crack. That would explains how we can have fiber breaks when the failure strain of fibers is 7%.

The stress level required to create the macroscopic transverse crack depends on the interface quality and on porosity. High porosity increases stresses locally and also in average. Consequently, the composite would require lower applied stress which is reflected in data in Table 10.

In cases when these cracks form:

- higher V_f would lead to larger total area with weak interface;
- higher fiber radius would make debond growth easier (fracture mechanics);
- porosity would be important enhancing mechanism (stress concentrations, higher average stress in the crack plane).

Table 9. Strength change with fiber volume fraction change: wood fiber composites.

Fiber type	$V_v(60)/V_v(40)$	$V_f(60)/V_f(40)$	$\sigma_c(60)/\sigma_c(40)$
Birch	1.5	1.39	1.30
Softwood	1.5	1.37	1.29
Eucalyptus viminalis	2.6	1.19	1.23

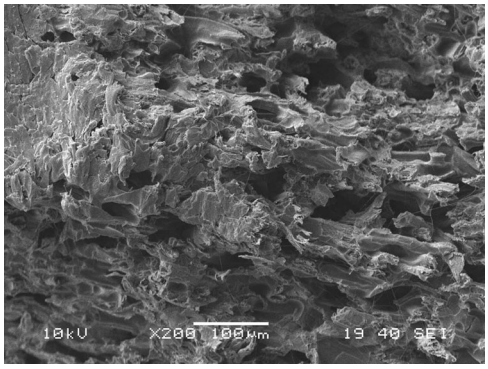

Figure 8. SEM images of softwood/PLA composite fracture surface with W_f= 40%. Failure surface crossing clusters of "fines".

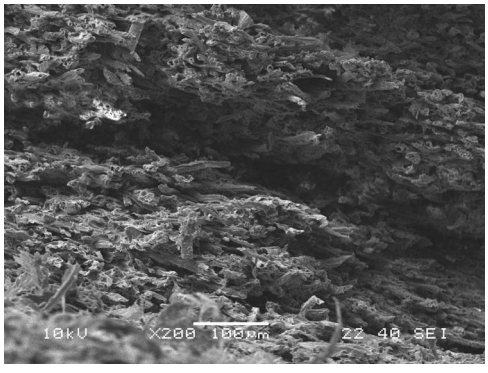

Figure 9. SEM images of *Eucalyptus viminalis*/PLA composite fracture surface with W_f = 60%.

Table 10. Strength change with fiber volume fraction: Tencel fiber composites.

Fiber type	$V_v(60)/V_v(40)$	$V_f(60)/V_f(40)$	$\sigma_c(60)/\sigma_c(40)$
1.7 dtex 3 mm Tencel	1	1.54	1.27
1.7 dtex 4 mm Tencel	1.6	1.34	1.24
1.7 dtex 6 mm Tencel	1.9	1.25	0.92
2.4 dtex 6 mm Tencel	2.3	1.15	0.85

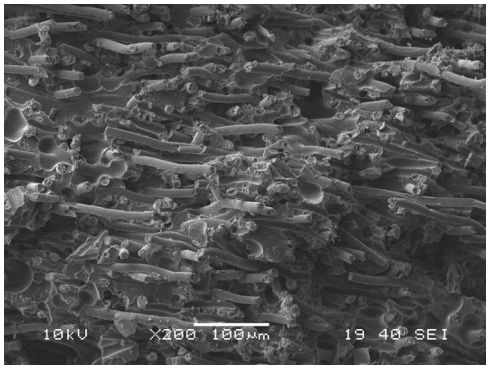

Figure 10. SEM micrograph of W_f = 60% Tencel 1.7 dtex 6 mm composite fracture surface.

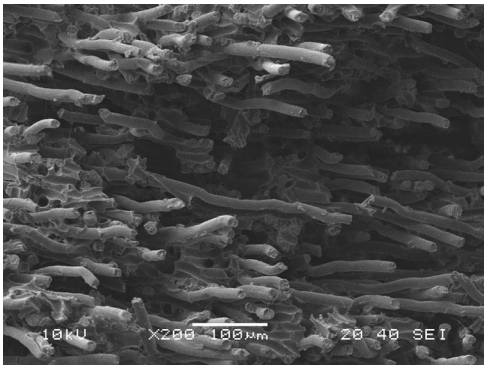

Figure 11. SEM micrograph of W_f = 40% Tencel 2.4 dtex 6 mm composite fracture surface.

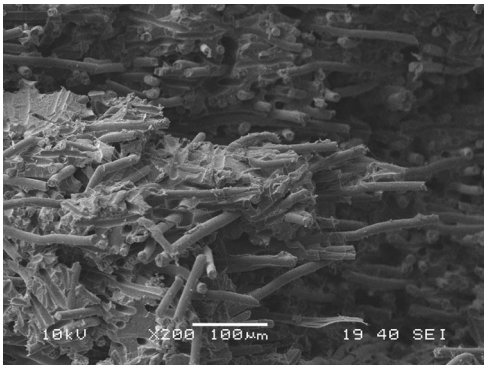

Figure 12. SEM micrograph of W_f = 40% Tencel 1.7 dtex 3 mm composite fracture surface.

From SEM micrographs, it seems that longer fibers tend to make local clusters with similar fiber orientation, phenomenon which becomes more pronounced for thick fibers, see Figure 11. Shorter fibers behave more "individually" making creation of a well-defined transverse crack more difficult or even impossible, see Figure 12. It is possible that well-defined cracks of the described nature are even not forming in 3- and 4-mm fiber composites.

Conclusion

Three wood fiber composites with PLA matrix and man-made cellulosic (Tencel) fiber/PLA composites with four fiber configurations have been produced using dynamic sheet former and analyzed using SEM, CT and tensile testing. The effect of the fiber/matrix weight content change on mechanical behavior (elastic modulus and strength) of composites has been investigated and possible explanations of sometimes peculiar behavior are suggested. For example, increasing fiber weight content in 6-mm Tencel fiber composites caused modulus and strength reduction.

Analyzing test results and applying several models (shear lag model with- and without porosity), distinct difference in stress transfer mechanisms is suggested between wood- and Tencel fiber composites. It is speculated that in wood fiber composites the fiber/fiber interaction is an important mechanism that together with fiber/matrix interaction and high porosity defines the stiffness and strength of these composites.

In Tencel fiber composites, the fiber/fiber interaction seems to be negligible due to circular cross-section of these fibers.

Based on the available data, it is speculated that in spite of all fibers having high aspect ratio (they can be considered as long fibers), the actual fiber length and width are important parameters: fibers that are shorter and thinner have larger flexibility and orientation adjustment ability. It may lead to increasing contact area with other fibers in wood fiber composites, leading to higher modulus and strength of wood composites. In shortest, Tencel fiber composites variation in orientation reduces the probability of creating clusters of certain off-axis fiber orientation observed as typical for longer fibers. In the latter case, weak fiber/matrix interface leads to large debonds forming on off-axis fiber surface. Coalescing with voids, they may build macro-crack which would be the triggering mechanism for Tencel fiber composite failure.

Acknowledgments

Erasmus students Benjamin Schamme and Quentin Viel from University of Rouen are acknowledged for their help in testing. We are grateful to Kristina Junel, Rise Bioeconomy, who produced the tested composites.

Disclosure statement

No potential conflict of interest was reported by the authors.

References

Abdennadher, A., Vincent, M. and Budtova, T. (2016) Rheological properties of molten flax- and Tencel®-polypropylene composites: Influence of fiber morphology and concentration. *Journal of Rheology*, 60(1): 191–201.

Abdullah, I., Blackburn, R. S., Russell, S. J. and Taylor, J. (2006) Tensile and elastic behavior of Tencel continuous filaments. *Journal of Applied Polymer Science*, 99(4): 1496–1503.

Adusumali, R.-B., Reifferscheid, M., Weber, H., Roeder, T., Sixta, H. and Gindl, W. (2006) Mechanical properties of regenerated cellulose fibres for composites. *Macromolecular Symposia*, 244: 119–125.

Agarwal, B. D. and Broutman, L. J. (1990) *Analysis and Performance of Fiber Composites*. 2nd edition (New York: John Wiley & Sons Inc).

Arganda-Carreras, I., Kaynig, V., Rueden, C., Eliceiri, K. W., Schindelin, J., Cardona, A. and Sebastian Seung, H. (2017) Trainable WEKA segmentation: A machine learning tool for microscopy pixel classification. *Bioinformatics (Oxford, England)*, 33(15): 2424–2426.

Bajpai, P. K., Singh, I. and Madaan, J. (2014) Development and characterization of PLA-based green composites: A review. *Journal of Thermoplastic Composite Materials*, 27(1): 52–81.

Bledzki, A. K. and Gassan, J. (1999) Composites reinforced with cellulose based fibres. *Progress in Polymer Science (Oxford)*, 24(2): 221–274.

Du, Y., Wu, T., Yan, N., Kortschot, M. T. and Farnood, R. (2014) Fabrication and characterization of fully biodegradable natural fiber-reinforced poly(lactic acid) composites. *Composites Part B: Engineering*, 56: 717–723.

Eichhorn, S. J., Baillie, C. A., Zafeiropoulos, N., Mwaikambo, L. Y., Ansell, M. P., Dufresne, A., Entwistle, K. M., Herrera-Franco, P. J., Escamilla, G. C., Groom, L., Hughes, M., Hill, C., Rials, T. G. and Wild, P. M. (2001) Review: Current international research into cellulosic fibres and composites. *Journal of Materials Science*, 36(9): 2107–2131.

Fekete, E., Kun, D. and Móczó, J. (2018) Thermoplastic starch/wood composites: Effect of processing technology, interfacial interactions and particle characteristics. *Periodica Polytechnica Chemical Engineering*, 62(2): 129–136.

Gamstedt, K. E. (1997) *Fatigue Damage Mechanisms in Polymer Matrix, Composites*. Thesis (PhD), Luleå University of Technology.

Hildebrand, T. and Rüegsegger, P. (1997) A new method for the model-independent assessment of thickness in three-dimensional images. *Journal of Microscopy*, 185(1): 67–75.

Jähne, B. (2004) *Practical Handbook on Image Processing for Scientific and Technical Applications* (New York: CRC Press).

Kellogg, R. M. and Wangaard F. F. (1969) Variation in the cell-wall density of wood. *Wood and Fiber Science*, 3: 180–204.

Krenchel, H. (1964) *Fibre Reinforcement: Theoretical and Practical Investigations of the Elasticity and Strength of Fibre-reinforced Materials* (Copenhagen: Academisk Forlag).

Lilholt, H. and Lawther, J. M. (2000) Natural organic fibres. In A. Kelly and C. Zweven (eds.) *Comprehensive Composite Materials*, Vol 1 (New York: Pergamon Press).

Madhavan Nampoothiri, K., Nair, N. R. and John, R. P. (2010) An overview of the recent developments in polylactide (PLA) research. *Bioresource Technology*, 101(22): 8493–8501.

Madsen, B. and Lilholt, H. (2003) Physical and mechanical properties of unidirectional plant fibre composites – an evaluation of the influence of porosity. *Composites Science and Technology*, 63(9): 1265–1272.

Madsen, B., Thygesen, A. and Lilholt, H. (2009) Plant fibre composites – porosity and stiffness. *Composites Science and Technology*, 69(7–8): 1057–1069.

Madsen B, Joffe, R., Peltola, H. and Nättinen, K. (2011) Short cellulosic fiber/starch acetate composites – micromechanical modeling of Young's modulus. *Journal of Composite Materials*, 45(20): 2119–2131.

Marklund, E., Varna, J. and Wallström, L. (2006) Nonlinear viscoelasticity and viscoplasticity of flax/polypropylene composites. *Journal of Engineering Materials and Technology, Transactions of the ASME*, 128 (4): 527–536.

Mertens, O., Gurr, J. and Krause, A. (2017) The utilization of thermomechanical pulp fibers in WPC: A review. *Journal of Applied Science*, 134(31): article no. 45161.

Migneault, S., Koubaa, A., Erchiqui, F., Chaala, A., Englund, K. and Wolcott, M. P. (2009). Effects of processing method and fiber size on the structure and properties of wood-plastic composites. *Composites Part A: Applied Science and Manufacturing*, 40(1): 80–85.

Mott, L., Groom, L. and Shaler, S. (2002) Mechanical properties of individual southern pine fibers: Part II. Comparison of earlywood and latewood fibers with respect to tree height and juvenility. *Wood and Fiber Science*, 34(2): 221–237.

Neagu, C. (2006) *Hygroelastic behaviour of wood-fibre based materials on the composite, fibre and ultrastructural level*. Thesis (PhD), Royal Institute of Technology.

Neagu, R. C., Gamstedt, E. K. and Berthold, F. (2006) Stiffness contribution of various wood fibers to composite materials. *Journal of Composite Materials*, 40(8): 663–699.

Nyström, B. (2007) *Natural fiber composites. Optimization of microstructure and processing parameters*. Thesis (Licentiate), Luleå University of Technology.

Pupure, L., Varna, J., Joffe, R. and Pupurs A. (2013) An analysis of the nonlinear behavior of lignin-based flax composites. *Mechanics of Composite Materials*, 49(2): 139–154.

Pupure, L., Doroudgarian, N. and Joffe, R. (2014) Moisture uptake and resulting mechanical response of biobased composites. I. Constituents. *Polymer Composites*, 35(6): 1150–1159.

Pupure, L., Varna, J. and Joffe, R. (2015) On viscoplasticity characterization of natural fibres with high variability. *Advanced Composites Letter*, 24(6): 125–129.

Raghu, N., Kale, A., Raj, A., Aggarwal, P. and Chauhan, S. (2018) Mechanical and thermal properties of wood fibers reinforced poly(lactic acid)/thermoplasticized starch composites. *Journal of Applied Polymer Science*, 135(15): article no. 46118.

Sjöström E. (1993) *Wood Chemistry – Fundamentals and Applications* (San Diego: Academic Press).

Spiridon, I., Darie, R. N. and Kangas, H. (2016) Influence of fiber modifications on PLA/fiber composites. Behavior to accelerated weathering. *Composites Part B: Engineering*, 92: 19–27.

Varna, J., Rozite L., Joffe R. and Pupurs A. (2012). Non-linear behaviour of PLA based flax composites. *Plastics, Rubber and Composites*, 41(2): 49–60.

Wambua, P., Ivens, J. and Verpoest, I. (2003). Natural fibres: Can they replace glass in fibre reinforced plastics? *Composites Science and Technology*, 63(9): 1259–1264.